An Equitable Active Power Curtailment Framework for Overvoltage Mitigation in PV-rich Active Distribution Networks

Eihab E.E. Ahmed *Graduate Student Member, IEEE*, Alpaslan Demirci *Member, IEEE*, Gokturk Poyrazoglu *Senior Member, IEEE*, and Saaed D. Manshadi *Senior Member, IEEE*

***Abstract*—There are various active power curtailment (APC) approaches to mitigate overvoltage. In PV-rich networks, the overvoltage happens to be especially at the end of the distribution feeders. While APC helps maintain voltage within operational limits, it results in varying degrees of renewable curtailment for each prosumer. This curtailment increases as the distance from the transformer grows. Hence, these approaches introduce unfairness among prosumers. This study proposes an equitable APC (EAPC) based on the prosumer's self-consumption rate (SCR). The method calculates each prosumer's SCR, compares it with the precalculated critical SCR, and calculates a fair share of curtailment for each prosumer. Subsequently, leveraging the voltage sensitivity matrix obtained from the inverse of the Jacobian matrix, the new active power injection at the point of common coupling (PCC) is calculated to mitigate the overvoltage. To show the effectiveness of the proposed method, a comparison with three other methods is presented under various PV penetration levels. The proposed EAPC is less sensitive to the prosumer's location and improves fairness among prosumers. In addition, a battery deployment scenario is analysed considering the annual supply and demand balance to suppress the extra curtailment introduced by EAPC without increasing the battery capacity.**

***Index Terms*—PV systems, active power control, overvoltage mitigation, Fairness, self-consumption rate.**

I. Introduction

In recent years, PV systems have emerged as a crucial component that facilitates global efforts to reduce dependence on fossil fuels and mitigate the adverse impact of climate change. By harnessing solar energy, PV systems offer a renewable and abundant source of electricity generation, thereby decreasing reliance on finite and environmentally harmful fossil fuel resources. The advantages of PV systems are manifold, ranging from their ability to generate electricity without emitting greenhouse gases or other pollutants to their scalability and modularity for ease of installation, making them suitable for diverse applications ranging from residential rooftops to large-scale utility installations. Additionally, PV systems can contribute to decentralized energy production, empowering communities to become more self-sufficient and resilient against disruptions in centralized power grids [1]–[3].

However, despite their numerous benefits, integrating PV systems into existing power grids poses significant technical challenges. One of the foremost issues is the intermittency of solar energy, which can lead to mismatches between supply and demand and increase voltage fluctuations within low-voltage (LV) distribution networks [4]. Furthermore, the non-dispatchable nature of solar power presents operational challenges for grid operators. The intermittent generation from PV systems is compensated with the stable output of conventional power plants to ensure grid stability and reliability. Additionally, the spatial distribution of PV installations, often concentrated in areas with high solar irradiance, may result in voltage rise issues in distribution networks with high PV penetration levels, necessitating careful planning and management strategies [5], [6]. Moreover, the integration of PV systems into power grids requires the deployment of advanced monitoring, control, and communication technologies to facilitate real-time management of generation and consumption patterns [7].

Conventional power grids were designed to serve the end users by assuming the unidirectional power flow concept from the upstream grid to the downstream end users. Nevertheless, deploying distributed PV systems may present a power flow from the end-users to the upstream grid when the local supply surpasses the local demand or when the demand is reduced to the point of overgeneration. Resultant reverse power flow causes increased voltage and power losses [8]–[11]. Besides the supply-demand balance, other factors may also cause overvoltage, especially at the end of the feeder, such as feeder impedance and network configuration [12]. In response to such conditions, inverters can take some action to mitigate overvoltage. Although some smart inverters can curtail a portion of the generation by the mismatch in available DC-generated PV and what the inverter delivers to the grid, generally one of the solutions is to have inverters programmed to disconnect from the grid temporarily and then reconnect after a delay when the voltage at the PCC exceeds the maximum voltage threshold. [13]. However, this frequent switching can disrupt the smooth operation of the network and potentially compromise its stability [14]. Therefore, several control mechanisms were introduced to address the technical issues and ensure the seamless integration of PV systems into the power grid.

Utilities are regulating the amount of power injected into the grid from PV systems by the operators to mitigate overvoltage issues and maintain grid stability. Such control strategies may involve reactive power control (such as volt-var) [15]–[18], active power control (volt-watt) [19]–[22], or both of them

Manuscript received x; revised x.

[23]–[27]. Specifically, deployment of on-load tap changing transformers, voltage regulators, and grid reinforcement applications could be applied to address overvoltage problems [28]–[30]. Reactive power control is based on the relationship between the reactive power and voltage magnitude in transmission networks. Unlike transmission networks, LV distribution networks have a relatively high resistance-to-reactance (R/X) ratio, making the voltage more sensitive to active power variations. Hence, reactive power control has a limited impact on voltage in LV distribution networks and could alleviate the problem to some extent [31]–[33]. Instead, APC is more attractive and would still be required given such a high R/X ratio [24].

The literature is rich in the two APC methods: distributed APC and centralized APC. Distributed APC methods are generally droop-based and do not necessitate a communication infrastructure, simplifying their implementation process significantly. In contrast, centralized APC involves communication links. A central unit is responsible for computing active and reactive power set-points for the inverters and sending real-time signals. Therefore, centralized approaches require more intricate and communication connections [25], [34].

Although APC methods can mitigate overvoltage, they introduce a fairness issue among prosumers based on the financial benefits due to the radial layout of typical LV distribution networks, wherein prosumers located farther from the substation encounter voltage rise during periods of reverse power flow when supply exceeds demand [35]. Consequently, APC applies higher degrees of renewable curtailment to prosumers, particularly those at the feeders' end, thereby reducing their potential benefits.

In this study, fairness is defined as the capability of the control method to treat prosumers equitably based on their power injection into the grid and self-consumption rate (SCR), irrespective of their location within the network. In other words, the location of the prosumer within the grid should not significantly affect the amount of curtailment and should not be used to penalize the prosumer. Some relevant studies on APC for overvoltage mitigation are summarized in Table I.

One of the suggestions to increase fairness is the previous schemes outlined in [31], [36]–[38]], which similar to our work, aim to limit the impact of location on curtailment. These papers implement a uniform generation limit for all PV systems, expressed as a percentage of PV's rated installed capacity. However, while simple to implement, this approach may not uphold fairness when assessing the prosumer's net demand, potentially curtailing households even if their PV generation doesn't contribute to the overvoltage, unlike our SCR-aware approach. In [56], an egalitarian fairness scheme is presented. This approach, like ours, aims for an equitable distribution of curtailment burden. However, it focuses on curtailing energy equally between customers, which can result in suboptimal outcomes. It exhibits the worst performance in terms of curtailment amount when compared to financial and proportional approaches because it ignores import/export factors and overlooks customers' net demand and PV installed capacity, unlike our method which considers individual SCR values for a more nuanced assessment. In [20], [25], [50], [51], the issue of unfair APC is tackled using local control strategies. While beneficial for minimizing communication infrastructure, these independent approaches suffer from a lack of coordination, neglecting the impact of active power injection from other nodes on voltage rise. This can leads to suboptimal curtailment decisions due to inadequate observability of the LVDN. In contrast, our proposed EAPC framework addresses this limitation by employing a centralized control scheme that incorporates real-time grid data and individual SCR values, enabling a coordinated, system-wide approach to equitable curtailment.

To overcome the coordination issue in local control, a droop-based APC strategy is introduced in [20], [50]. Similar to our method, these approaches use a voltage sensitivity matrix to guide curtailment. However, they utilize unique but fixed droop parameters for each inverter to ensure fair PV harvesting, which increases computational complexity and still relies on potentially inaccurate assumptions about uniform load profiles. This can cause inequitable curtailment scenarios, as it does not account for the diverse load profiles of households connected to the LVDN. Our EAPC method bypasses these limitations by dynamically adjusting curtailment based on real-time SCR and grid conditions.

As a solution for the coordinated operation between the participants, some studies implemented OPF-based centralized approaches [22], [52], [55]. These centralized approaches, like ours, benefit from enhanced observability of the LVDN and the potential for more equitable PV curtailment. However, OPF-based methods, while powerful, can become computationally intensive, especially with a large number of DERs in the LVDN due to the complexity of the optimization process. This has motivated us to explore alternative methods like EAPC, which achieve a balance between computational efficiency and fairness. Other control schemes presented in [53], [54] use distributed control, offering a compromise between the simplicity of local methods and the coordination of centralized schemes. These approaches aim for fairness but often face similar computational challenges as OPF-based solutions. Furthermore, they may not explicitly consider individual prosumer behavior like our SCR-aware EAPC method does.

Moreover, to prevent voltage instability, the studies [34], [39], [40] utilize a voltage sensitivity matrix to determine the PV power curtailment at each bus, as our method does. These approaches allow more energy injection into the grid than the droop-based approach. However, these strategies primarily consider the location to guide curtailment, disregarding the prosumer's SCR and overlooking the reality that a prosumer who can effectively synchronize their electricity consumption with solar generation during peak sunlight hours will only contribute minimal power to the grid, which is a key consideration in our EAPC framework.

Other methods employing fixed feed-in power limits, such as in [37] and [38], offer a better alternative to APC. However, while easy to implement, setting these limits without considering real-time grid dynamics can be problematic. Setting them too conservatively can result in underutilization of the full PV potential, while setting them too high can lead to

TABLE I
SUMMARY OF LITERATURE REVIEW ON APC FOR OVERVOLTAGE MITIGATION

Ref	Method	Control Scheme	Modeling Technique	Criteria 1	Criteria 2	Criteria 3	Criteria 4
[20], [25], [50], [51]	Droop	Local	Voltage sensitivity matrix	×	×	✓	×
[38]		Local and distributed	Model-Free	×	×	✓	×
[52]	Optimization	Centralized	ACOPF	✓	×	✓	×
[36]		Local and centralized	QP+Sensitivity	-	×	✓	×
[53], [54]		Distributed	Lagrangian-Based	×	×	✓	×
[22]		Centralized	ACOPF	×	×	✓	×
[55]		Centralized	ACOPF	✓	×	✓	×
This work	Droop	Centralized	SCR+Voltage sensitivity matrix	✓	✓	✓	✓

* Criteria 1: Diverse load profile, Criteria 2: Incorporate SCR, Criteria 3: Equitable APC, Criteria 4: Location sensitivity analysis

voltage instability. Our EAPC method avoids these pitfalls by dynamically adjusting curtailment based on actual grid conditions and individual SCR values.

This study proposes an improved APC control method based on prosumers' SCR by leveraging the voltage sensitivity matrix. The original contributions of this article include the following:

1) A SCR-based equitable framework for active power curtailment is proposed, which significantly improves the fairness of prosumers while observing the nodal voltage limits

2) The proposed framework can equitably alleviate the location impact on energy curtailment leveraging SCR and the power-voltage sensitivity, even under high PV penetration levels.

3) The framework can achieve a comparable energy harvest per year as the dynamic active curtailment method without increasing BESS capacity.

The rest of this article is organized as follows: section II explains the issues associated with the existing APC methods. section III describes the proposed EAPC. section IV reports the simulation results, including a comparative analysis between the methods. A discussion on the performance of APC overvoltage mitigation methods is presented in section V. Finally, the conclusion is given in section VI.

II. PROBLEM STATEMENT

Several control techniques to address overvoltage mitigation, such as inverter tripping, fixed feed-in power limitation, dynamic APC, and a new proposed EAPC, will be discussed in this paper.

Inverter tripping is one of the overvoltage mitigation methods where the inverter disconnects from the grid if the voltage at the PCC exceeds the critical voltage limit and reconnects after a time delay [31]. Because overvoltage arises at nodes distant from the transformer, prosumers located at the end of the feeder are disadvantaged due to their placement [21]. Nonetheless, this control approach operates independently of communication infrastructure among prosumers, relying instead on local control and it is performed according to Eq (1).

$$P_{inj} = \begin{cases} P_{exc}, & V_i < V_{cri} \\ 0, & V_i \geq V_{cri} \end{cases} \tag{1}$$

where P_{inj} is the injected power (kW), P_{exc} is the excess power (kW), V_i is the voltage at PCC (p.u), and V_{cri} is the critical voltage (p.u).

The local PV generation impacts the demand patterns and might surpass the load several times during the peak generation periods. The conventional power grids were not planned to consider feed-in PV power. The main aim of feed-in power limitation is to increase the PV hosting capacity of the feeders and enhance the renewable energy mix within the overall energy landscape. However, the integration of PV can introduce technical challenges such as voltage fluctuations, transformer strain, and switcher malfunctions. Consequently, grid operators either restrict) or PV installation, such as in Thailand [41] (PV is limited by 15% of rating transformers), or implement maximum feed-in power limits as a preventative measure against these potential drawbacks. For instance, the utility in Germany restricts the power injection by 70% of the prosumer's nominal installed PV power [42]. It's important to note that feed-in limits do not consider grid dynamics like supply, demand, or voltage variations; instead, they solely restrict surplus power. Consequently, this approach may underutilize renewable energy during specific periods due to unnecessary curtailment, and it doesn't ensure operation within the voltage safety range. This study assumes that prosumers cannot feed more than 40% of their installed PV capacity into the grid [43].

$$P_{inj} = \begin{cases} P_{exc}, & P_{exc} < \alpha P_{PV\_nom} \\ \alpha P_{PV\_nom}, & P_{exc} \geq \alpha P_{PV\_nom} \end{cases} \tag{2}$$

The feed-in power is calculated according to Eq (2), where P_{PV_nom} is the nominal PV power (kW), and α is the feed-in coefficient, changing between zero and one. The high R/X ratio is one of the main factors limiting the reactive power impact on voltage regulation in LV distribution networks. Rather, the APC is more effective in mitigating the overvoltage. There are two APC approaches, namely, droop-based APC and dynamic APC (DAPC). Droop-based APC is desirable due to its simplicity because it does not demand shared information between prosumers. Instead, it depends on local control. However, this method is location-sensitive, causing unfair energy curtailment among the prosumers [44]. The curtailment starts when the nodal voltage reaches the threshold voltage V_{th} as shown in Eq (3), where m is the droop-coefficient and is calculated based on Eq (4). The injection is disabled when the voltage reaches the critical voltage (V_{cri}). Dynamic APC (DAPC) is also a centralized approach that aims to regulate voltage by adjusting the active power output of PV inverters. Unlike the fixed droop relationship in droop-based

APC, DAPC determines the amount of curtailment for each prosumer based on their contribution to the overvoltage. This is achieved using a voltage sensitivity matrix, which quantifies the relationship between changes in active power injection at a specific bus and the resulting voltage changes at all buses in the network, which will be discussed in the following section. The mathematical formulation of DAPC is available in [45].

$$P_{inj} = \begin{cases} P_{exc}, & V_i \leq V_{th} \\ P_{exc} - m\left(V_i - V_{th}\right), & V_{th} < V_i \leq V_{cri} \\ 0, & V_i > V_{cri} \end{cases} \tag{3}$$

$$m = \frac{P_{exc}}{V_{cri} - V_{th}} \tag{4}$$

The IEEE European Low Voltage Test Feeder is considered a benchmark for the analysis. This is a typical distribution network in Europe developed by IEEE. The test feeder has 906 nodes with 55 active nodes, as illustrated in Figure 1. It is assumed that all the customers in this LV distribution network are prosumers equipped with PV systems, and the total installed PV capacity is distributed among the prosumers based on their demand. The total installed PV capacity and SCR of each of the 55 prosumer is depicted in Figure 2. PV capacity varies from 1 kW up to 19.6 kW, and the SCR varies from 4.9% to 84.1%, with an average of 27.5%. The SCR is the ratio between the part of the PV generation directly transferred to the load and the total PV generation, as stated in Eq (5). Load and PV profiles are obtained from [57], [58].

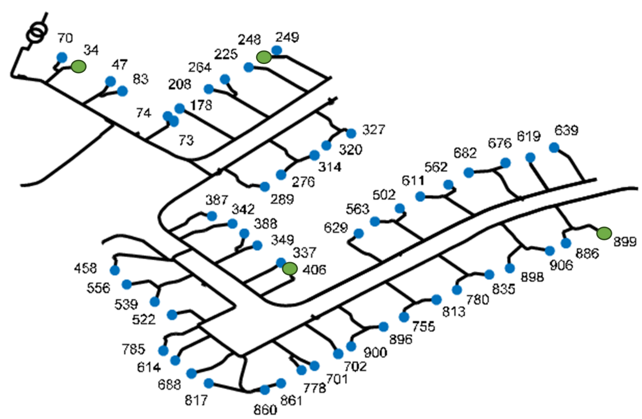

Fig. 1. Single-line diagram of the IEEE European LV distribution Test Feeder, green dots depict the examined nodes [57].

$$SCR = \frac{\int_{t=0}^{T} P_t^{pv \to load}}{\int_{t=0}^{T} P_t^{pv}} \tag{5}$$

where $P_t^{pv} = P_t^{pv \to load} + P_t^{pv \to grid} + P_t^{pv \to curtailed}$

Maximizing self-consumption is one of the main motivations behind PV installation for residential and industrial premises. High SCR levels are linked to technical and financial advantages. According to references [5], [47], a specific SCR threshold exists below which overvoltage issues arise in the LV distribution networks. Moreover, Reference [48] highlights the financial benefits of high SCR for residential end-users. Moreover, the secure voltage operational range of the LV distribution network is assumed to be between 0.94 and 1.10 p.u, and the transformer is configured at 1.05 p.u. A power flow simulation is performed using the time series demand and PV generation data with a 1-minute resolution by leveraging Pandapower [49].

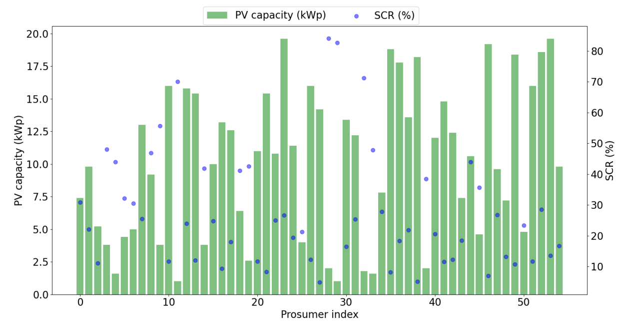

Fig. 2. PV installed capacity and SCR of the prosumers.

III. Proposed Equitable APC framework

As discussed in the previous sections, the APC methods disregard the prosumer's SCR, resulting in an inequitable energy curtailment among the prosumers. This study proposes an EAPC method that aims to enhance fairness among the prosumers by leveraging the SCR and voltage sensitivity while preserving the voltage under the critical voltage, V_{cri}. Prosumers will still adjust their active power at PCC, so their SCR should be greater than a predefined critical value, SCR_{cri}. The flowchart of the proposed EAPC method is depicted in Figure 3. The technique performs power flow calculation and computes the voltage sensitivity matrix. In the scenario when the maximum voltage in the network $V_i^{max} > V_i^{cri}$, each prosumer's SCR_t is calculated and compared to SCR_{cri} which is computed according to the algorithm in the pseudo-code. Subsequently, the prosumers SCR_t is adjusted by curtailing the surplus energy. In this way, the prosumers are penalized based on their SCR, therefore, the prosumers close to the transformer may experience energy curtailment based on their SCR. After that, the voltage sensitivity matrix is calculated and ΔP_i is computed and extracted from the prosumer's energy. The flowchart is elaborated in the following subsections.

A. Input data

The EAPC implementation algorithm necessitates solar and load profiles for each prosumer in the network. These profiles, which can be sourced from either forecast data or historical data typically obtained from smart meters, serve as inputs to the algorithm. Additionally, the algorithm requires inputs including the critical SCR, voltage operation limits, network configuration, and the desired time resolution.

B. Power flow and voltage sensitivity

The proposed method depends on the sensitivity matrix, which is the inverse of the power flow Jacobian matrix. This matrix is obtained by solving the AC power flow equations shown in Eqs (6-10).

$$P_{G_i} - P_{D_i} = \sum_{j=1}^{N} V_i.V_j.Y_{ij}.\cos\left(\theta_{ij} + \delta_j - \delta_i\right) \ , \quad \forall i, j \quad (6)$$

$$Q_{G_i} - Q_{D_i} = \sum_{j=1}^{N} V_i.V_j.Y_{ij}.\sin\left(\theta_{ij} + \delta_j - \delta_i\right) \ , \quad \forall i, j \quad (7)$$

$$I_{ij} = |Y_{ij}| . \Big[V_i^2 + V_j^2 - 2.V_i.V_j.\cos(\delta_{j,t} - \delta_i) \ \Big]^{1/2}, \quad \forall i, j \quad (8)$$

$$P_{loss} = \sum_{j=1}^{N} I_{ij}^2.r_{ij}, \quad \forall \ i, j \quad (9)$$

$$V_{min} \leq V_i \leq V_{max} \ , \quad \forall \ i \quad (10)$$

The active power flow is described in Eq (6), where P_{G_i} and P_{G_i} are the active supply and active demand in kW at bus i , respectively. Similarly, the reactive power flow is introduced in Eq (7), where Q_{G_i} and Q_{D_i} are the reactive supply and reactive demand, $\boldsymbol{V}_i = V_{\boldsymbol{i}}\angle\delta_i$ is the polar form of voltage at Bus i, V_i is the voltage magnitude at Bus i, δ_i is the voltage angle at Bus i, Y_{ij} and θ_{ij} are the admittance matrix amplitude and angle between bus i and bus j, respectively. The current flow between bus i and bus j is given in Eq (8). Meanwhile, the overall active power loss is calculated by Eq (9), where r_{ij} is the resistance of the line connecting bus i and j. The voltage operation limits are given in Eq (10), where V_{min}, and V_{max} are the voltage lower and upper boundaries, respectively. The correlation between voltage and power changes can be derived from the power flow analysis results according to the Newton-Raphson technique as shown in Eq (11) .

$$\begin{bmatrix} \Delta P \\ \Delta Q \end{bmatrix} = J \ . \ \begin{bmatrix} \Delta\delta \\ \Delta V \end{bmatrix} = \begin{bmatrix} \frac{\partial P}{\partial \delta} & \frac{\partial P}{\partial V} \\ \frac{\partial Q}{\partial \delta} & \frac{\partial Q}{\partial V} \end{bmatrix} \begin{bmatrix} \Delta\delta \\ \Delta V \end{bmatrix} \quad (11)$$

$$\begin{bmatrix} \Delta\delta \\ \Delta V \end{bmatrix} = J^{-1} \ . \ \begin{bmatrix} \Delta P \\ \Delta Q \end{bmatrix} =$$

$$\left[\begin{matrix} \underbrace{\begin{matrix} \frac{\partial \delta_2}{\partial P_2} & \cdots & \frac{\partial \delta_2}{\partial P_N} \\ \vdots & \ddots & \vdots \\ \frac{\partial \delta_N}{\partial P_2} & \cdots & \frac{\partial \delta_N}{\partial P_N} \\ \frac{\partial V_2}{\partial P_2} & \cdots & \frac{\partial V_2}{\partial P_N} \\ \vdots & \ddots & \vdots \\ \frac{\partial V_N}{\partial P_2} & \cdots & \frac{\partial V_N}{\partial P_N} \end{matrix}}_{V \ sen. \ at \ P} & \underbrace{\begin{matrix} \frac{\partial \delta_2}{\partial Q_2} & \cdots & \frac{\partial \delta_2}{\partial Q_N} \\ \vdots & \ddots & \vdots \\ \frac{\partial \delta_N}{\partial Q_2} & \cdots & \frac{\partial \delta_N}{\partial Q_N} \\ \frac{\partial V_2}{\partial Q_2} & \cdots & \frac{\partial V_2}{\partial Q_N} \\ \vdots & \ddots & \vdots \\ \frac{\partial V_N}{\partial Q_2} & \cdots & \frac{\partial V_N}{\partial Q_N} \end{matrix}}_{V \ sen. \ at \ Q} \end{matrix} \right] \begin{bmatrix} \Delta P \\ \Delta Q \end{bmatrix} \quad (12)$$

$$S_V = \begin{bmatrix} \frac{\Delta \delta}{dP} & \frac{\Delta \delta}{dQ} \\ \frac{\Delta V}{dP} & \frac{\Delta V}{dQ} \end{bmatrix} \quad (13)$$

The voltage sensitivity matrix quantifies how the changes in active and reactive power affect voltage magnitude $|V|$ and voltage angle δ. It is obtained by partial derivative of the power flow equations and taking the inverse of the Jacobian matrix, as given in Eqs (12-13). The sensitivity matrix S_V consists of 4 sub-matrices ($S_V^{m,n}$;m=1,2;n=1,2), however, EAPC method particularly utilizes the sub-matrix $\frac{\Delta V}{dP}$ because the voltage is more sensitive to active power variation in LV distribution network as discussed in the previous sections. Eq (14) calculates energy curtailment at each bus (ΔP_i) and Eq (15) calculates the droop coefficient (m_i).

$$\Delta P_i = \frac{V_i - V_i^{cri}}{\sum_i^N S_{V,i}^{2,1}} \quad (14)$$

$$m_i = \frac{\Delta P_i}{V_i - V_i^{cri}} \quad (15)$$

C. Critical self-consumption rate

The SCR_{cri} calculation algorithm comprises three functions. Function 1 computes the SCR of each prosumer using Eq (5), taking into account the PV and load profiles. Function 2 then receives the SCR from Function 1 and compares it against a specified threshold. If the SCR is below this threshold, the prosumer's energy is curtailed to elevate the SCR to the required level, and this function returns the difference between the original and adjusted PV generation. Finally, Function 3 determines SCR_{cri} by identifying the breakpoints from the energy curtailment data obtained. The first breakpoint occurs at an SCR of 3%, and the second breakpoint occurs at 12% as shown in Figure (4). The selection of a critical SCR has an impact on our two stages of energy curtailment. In the first stage, curtailment is based on the prosumer's SCR, while the second stage considers their voltage sensitivity coefficients. Setting a high SCR threshold would lead to unnecessary excessive curtailment. Meanwhile, a low threshold would disproportionately affect prosumers based on their location-dependent voltage sensitivities. Hence, an SCR of 3% (for the network under consideration) is a good choice to create a balance between ensuring equity and avoiding unnecessary curtailment.

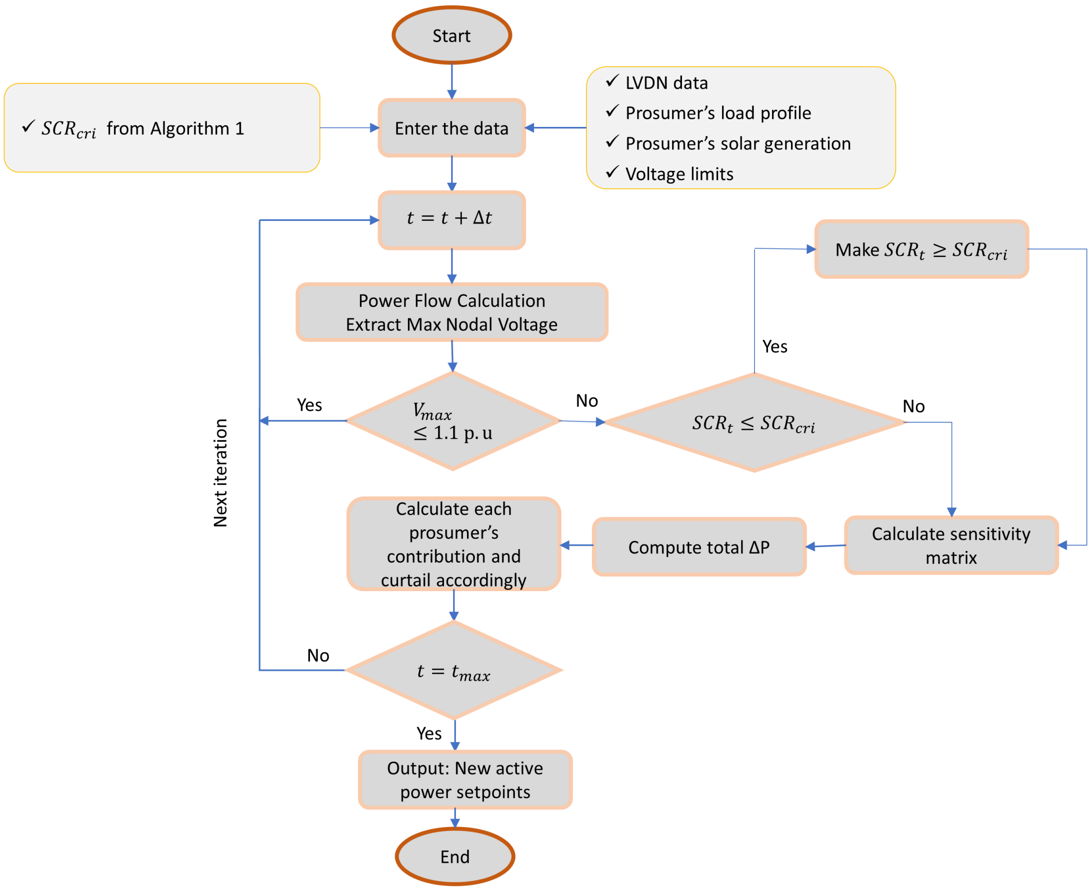

Fig. 3. Flow chart of the proposed EAPC.

Algorithm 1 Proposed Algorithm for Calculating the Critical SCR.

$\boldsymbol{Function1: \ Calculate \ SCR}$
  $\boldsymbol{Input}: \ P_{G_{i,t}}, \ P_{D_{i,t}}, \ N, T$
  $For \ each \ (i,t) \ in \ (N,T)$
    $\boldsymbol{Calculate} \ SCR_{i,t} \ based \ on \ (5)$
  $End \ For$
  $\boldsymbol{Output}: \ SCR_{i,t}$
$\boldsymbol{Function2}: Calculate \ Curtailment \ based \ on \ SCR$
  $\boldsymbol{Input}: \check{SCR}, \ P_{G_{i,t}}, \ P_{D_{i,t}}, \ N, T, SCR_{i,t}$
  $For \ each \ (i,t) \ in \ (N,T)$
    $If \ SCR_{i,t} < \check{SCR}$
      $P^{new}_{G_{i,t}} = \frac{P_{D_{i,t}}}{1 - SCR_{i,t}}$
    $Else$
      $P^{new}_{G_{i,t}} = P_{G_{i,t}}$
    $End \ If$
  $End \ For$
  $\boldsymbol{Compute} \ \overline{\in} = \sum_t^T \sum_i^N (P_{G_{i,t}} - P^{new}_{G_{i,t}})$
  $\boldsymbol{Output}: \ \overline{\in}$
$\boldsymbol{Function3: \ Determine \ SCR_{cri}}$
  $\boldsymbol{Input}: \widehat{SCR}, \ \overline{\ni}$
  $For \ \check{SCR} \ in \ \widehat{SCR}$
    $\overline{\in} \ = Function2(\check{SCR})$
    $\boldsymbol{Append} \ \overline{\in} \ to \ \overline{\ni}$
  $End \ For$
  $\boldsymbol{Plot}(\widehat{SCR}, \overline{\in})$
  $\boldsymbol{Detect} \ SCR_{cri}$
  $\boldsymbol{Output}: \ SCR_{cri}$

*$\check{SCR}$: Threshold of SCR; $\widehat{SCR}$: List of SCRs to be evaluated; $\overline{\in}$: Energy curtailment; $\overline{\ni}$: Empty list to store $\overline{\in}$.

Energy curtailment resulting from the SCR constraint leads to an enhancement in voltage profile even before implementing the sensitivity-matrix-based curtailment. This is because the total energy injected into the system is decreased. Consequently, when the sensitivity matrix is applied, location-based penalties are reduced compared to the scenario where the SCR constraint is neglected.

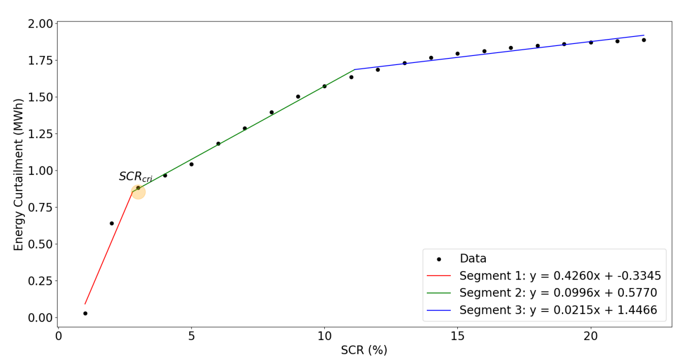

Fig. 4. Sensitivity of Energy curtailment to SCR.

IV. Performance evaluation

This section aims to validate the performance of the proposed EAPC by comparing it with the other overvoltage mitigation methods: DAPC, tripping, and feed-in power limitation. The technical comparison is conducted for a typical clear day, considering energy curtailment and nodal voltage variations under different PV penetrations.

A. Energy curtailment considering overall PV generation

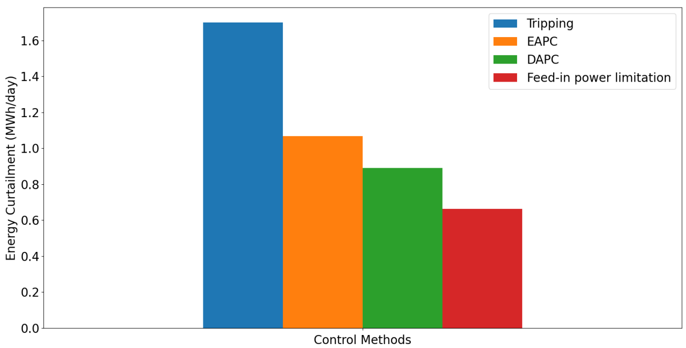

Fig. 5. The amount of energy curtailment for a typical clear day

A comparative analysis of four techniques for energy curtailment for a typical clear day is illustrated in Figure 5. The maximum energy curtailment of 1.7 MWh occurs under the tripping method because the inverter disconnects from the PCC when experiencing overvoltage cases; thereby, 56.6% of the total PV generation is curtailed. The proposed EAPC and DAPC energy curtailments are 1.05 MWh and 0.9 MWh, respectively. This correspondence to a curtailment difference of less than 0.4% when considering the total surplus energy of 44 MWh. As we will discuss later, the feed-in power method has the minimum energy curtailment; however, this control method does not guarantee voltage stability for higher PV penetrations. Furthermore, EAPC and DAPC would achieve less energy curtailment if the feed-in power limit drops below 40%.

B. Nodal voltage fluctuations

The nodal voltage fluctuations are analysed considering the base case (no power control) and the other four power control techniques as shown in Figure 6. Four buses are selected to display the results while considering their electrical distance from the substation: Bus 34, Bus 248, Bus 406, and Bus 899. The smaller the bus number, the closer to the substation. At Bus 34 (Figure 6. A), the voltage doesn't exceed the extreme operation condition (1.1 pu). Thus, the inverter remains connected to the PCC. However, the voltage drops at bus 34 due to the inverter tripping at different buses, especially the ones at the end of the feeder. Furthermore, the maximum voltage at buses 248, 406, and 899 occurs at noon, and the highest power injection is associated with Feed-in power, DAPC, EAPC, and tripping, respectively. Consequently, the rise in voltage corresponds proportionally to the increase in power injection. Therefore, it can be inferred that the method exhibiting the highest power injection will also undergo the most substantial voltage rise. It is worth mentioning that the voltage rises as the distance from the substation increases. Therefore, the maximum voltage in the system (1.16 pu) is recorded at the end of the feeder at bus 899.

TABLE II
Energy curtailment rates by power curtailment methods

Method	Bus 34	Bus 248	Bus 406	Bus 899
DAPC	8%	58.8%	31.5%	24.3%
EAPC	29.7%	16%	12%	18.3%
Feed-in power	18.6%	6%	17.7%	22.4%
Tripping	0%	21.9%	56.4%	62.2%

C. Energy curtailment considering nodal PV generation

The energy curtailment at the selected buses after applying power control methods is given in Table II. The total solar generation at Bus 34 is 40 kWh. After implementing DAPC, EAPC, feed-in power, and tripping methods, the usable solar generation has dropped to 36.8 kWh, 28.1 kWh, 32.6 kWh, and 40 kWh. It can be observed from Figure 6 that the voltage at bus 34 is below V_i^{max}; thus, the inverter remains connected to the grid. This case leads to the solar generation at bus 34 being the same as the base case under the ripping method, without energy curtailment. At buses 248, 406, and 899; the total generation is 20.4 kWh, 58.2 kWh, and 100 kWh, respectively. The curtailed energy at these buses due to DAPC is 58.8%, 31.5%, and 24.3%. When considering the feed-in power limit, the energy curtailment rates are 18.6%, 6%, 17.7%, and 22.4%, corresponding to total utilizable solar energy of 32.4 kWh, 39 kWh, and 36.4 kWh at bus 248, 406, and 899, respectively. Furthermore, the usable solar energy used in the tripping method for the same buses is 16 kWh, 25.4 kWh, and 37.8 kWh, respectively. The prosumers at Bus 248 and 406 maintain a satisfactory SCR value, consistently exceeding the SCR_{cri} threshold most of the time. Consequently, the EAPC method demonstrates minimal energy curtailments (16% and 12% of total PV generation) compared to DAPC and tripping approaches, with most of the curtailment attributable to the location.

D. Energy curtailment considering location-sensitivity

As the prosumer moves farther from the distribution substation, more energy is curtailed under DAPC because prosumers at the end of the feeder are more vulnerable to overvoltage problems. This phenomenon is observed when changing the prosumer's location from near to the substation toward the end of the feeder, as seen in Table III. The energy curtailment increases from 8% at the beginning of the feeder to 56.7% at the end of the feeder. Thus, the usable solar generation starts from 100% under no control method and declines gradually to a minimum value of 43.3%. This means that moving Prosumer 1 from bus 34 to bus 899 leads to losing 22.7 kWh of its energy. On the contrary, energy curtailment rates change within a tiny range from 29.7% to 30.8% under EAPC. Hence, it could be stated that the EAPC method is less sensitive to the prosumer's site and is more affected by the SCR.

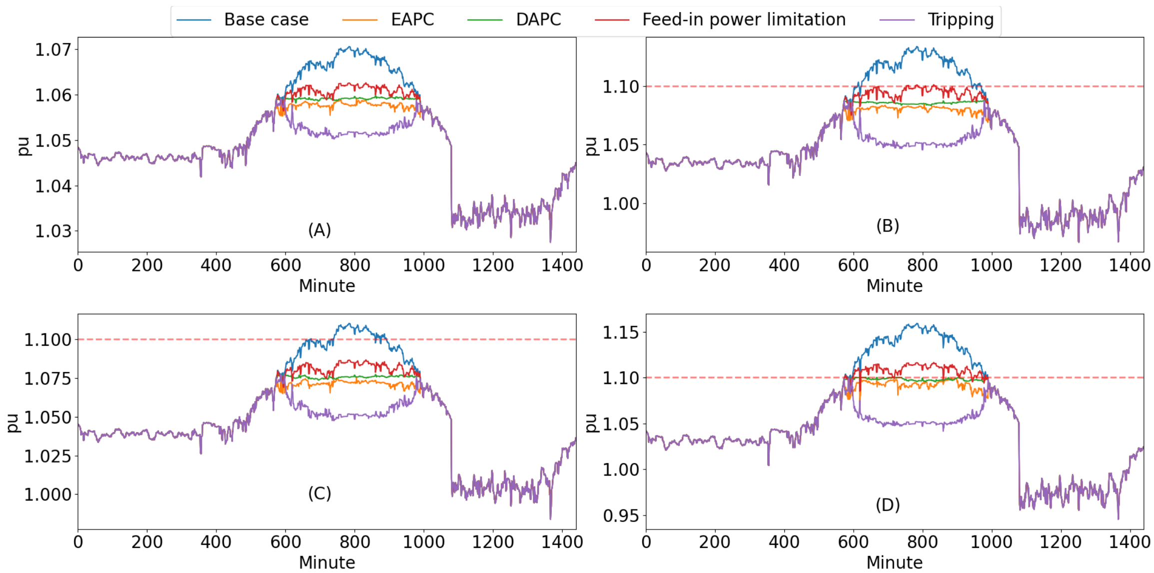

Fig. 6. The voltage variation after applying control methods at (A) bus 34, (B) bus 248, (C) bus 406, and (D) bus 899.

TABLE III
ENERGY CURTAILMENT RATES CONSIDERING LOCATION SENSITIVITY.

Method	Bus 34	Bus 248	Bus 406	Bus 682	Bus 899
DAPC	8%	32%	35.6%	52.6%	56.7%
EAPC	29.7%	29.9%	30.7%	30.8%	30.5%

E. Energy curtailment considering PV penetration

The impact of increasing PV penetrations on energy curtailment is analysed in Figure 7. The Figure has been obtained by increasing the total installed PV capacity in the distribution network, running power flow, and calculating the respective energy curtailment for each method. In area (A), DAPC, EAPC, and tripping achieved the least energy curtailment. The tripping method is the simplest and needs no information shared between participants, so it is recommended that it be applied for solar-to-demand ratios (PV penetrations) less than 60%. Nonetheless, in area (B), DAPC was associated with the least energy curtailment; however, the feed-in power limitation method achieved better energy savings than the tripping method for penetration levels greater than 70%. Feed-in power limitation outperformed other methods for penetration levels greater than 90%, as illustrated by area (C). Nevertheless, this method does not consider voltage stability and might lead to overvoltage problems in high PV penetrations, as shown in Fig 8. Additionally, there is a slight difference between DAPC and EAPC in area (c); however, the merit of EAPC lies in its fairness compared to DAPC, rendering it more suitable for implementation at penetration levels higher than 130%. These results will assist the grid operators in making a wise decision when selecting the curtailment method. Figure 8 shows the voltage rise in response to increased PV penetration when implementing the feed-in power limitation method. Bus 34 does not experience overvoltage problems despite the high PV penetration levels. On the other hand, as we move further from the substation, overvoltage occurs at lower penetration levels. For example, overvoltage occurs for penetration levels greater than 140%, 110%, and 80% at Bus 248, 406, and 899, respectively. Hence, it can be deduced that this approach becomes invalid as a power control mechanism beyond a specific penetration threshold. Instead, it is advisable to adapt the feed-in power limit according to the fluctuations in supply and demand.

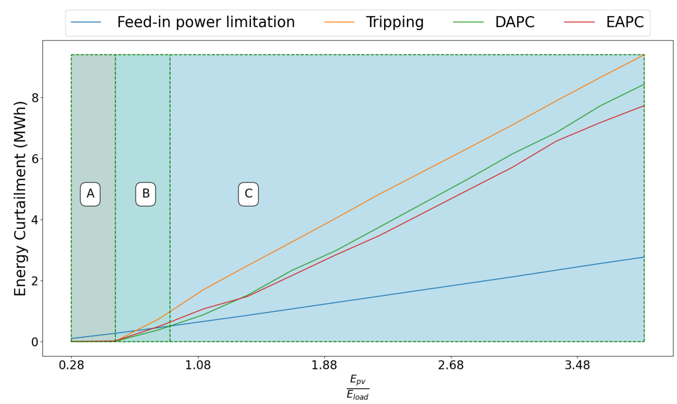

Fig. 7. Comparison of energy curtailment under different solar-to-demand ratios.

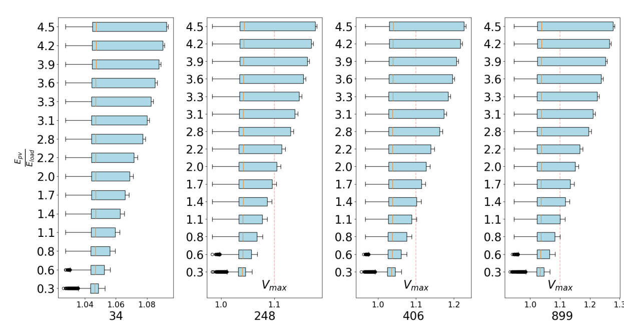

Fig. 8. Voltage fluctuations for different solar-to-demand ratios under feed-in power limitation.

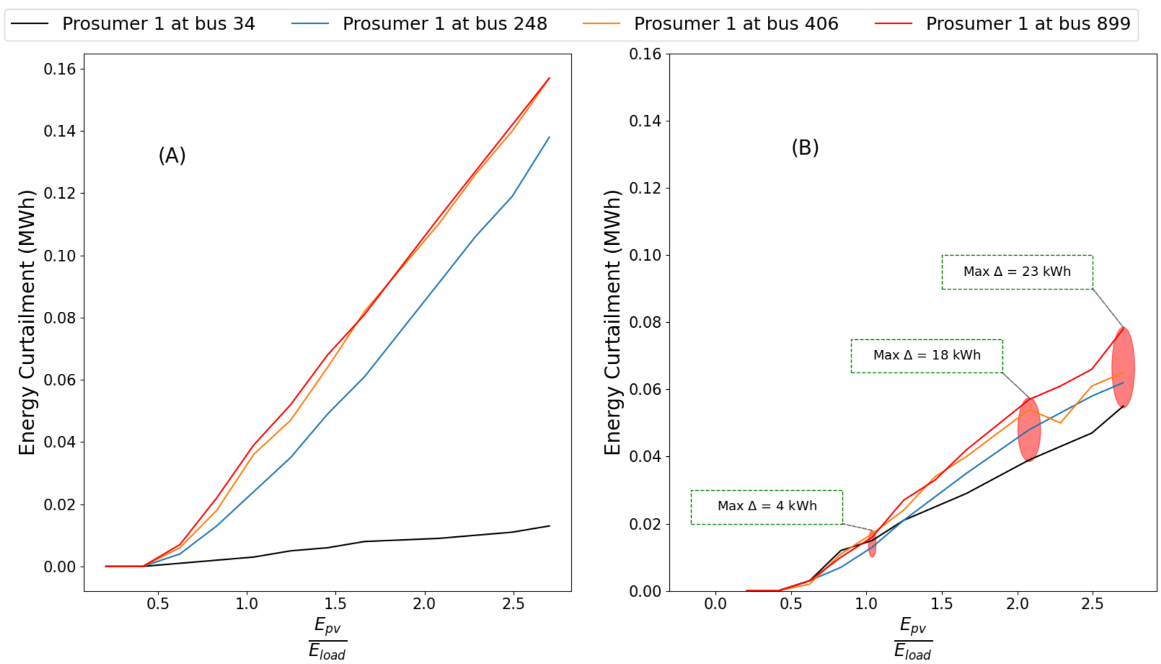

Fig. 9. Energy curtailment under increasing penetration level for a) DAPC and B) EAPC methods.

F. Energy curtailment considering location sensitivity and PV penetration

To reveal the correlation between energy curtailment and the prosumer's location, Prosumer 1 has been relocated from the vicinity of the substation (Bus 34) towards the terminus of the feeder (Bus 899) as shown in Figure 9. As mentioned before, DAPC is highly sensitive to the prosumer's location in the network. It can be noticed that despite the massive increase in the penetration level, the energy curtailment at Bus 34 slightly increases compared to the energy curtailment at buses further from the substation, where the energy curtailment increases dramatically. For instance, under a penetration level of 207%, the difference between energy curtailment at Bus 34 and 899 is more than 100 kWh. On the other hand, this difference (illustrated by Δ) is only 18 kWh in the case of EAPC, as shown in Figure 6.B. Since EAPC is based on SCR, the energy curtailment at bus 34 when applying EAPC is much higher than it when applying DAPC. However, the overall energy curtailment in EAPC is less than that of DAPC. This graph illustrates the superiority of EAPC over DAPC in terms of equitable energy curtailment.

G. Energy curtailment considering BESS

As the BESS capacity increases, there is a notable decrease in energy curtailment till a certain point. Figure 10 illustrates this consistent trend across all four methods. This phenomenon can be attributed to the capability of BESS to store surplus energy and subsequently release it during peak demand periods. Doing so diminishes the need to curtail energy production, resulting in a more efficient utilization of resources and reduced wastage. The difference in energy curtailment between DAPC and EAPC can be further reduced using BESS, as shown in the graph. For example, for a BESS capacity of 2.5 MWh, there is about 1.6% energy curtailment decrease when applying EAPC compared to DAPC. Noteworthy, the capacity of the Battery Energy Storage System (BESS) is determined by assessing both annual demand and supply. In the region under examination, where cloudy or partially cloudy weather conditions characterize 131 days, the total energy curtailment experiences a notable decrease. Furthermore, this reduction in curtailment will be even more pronounced in regions with greater cloud cover.

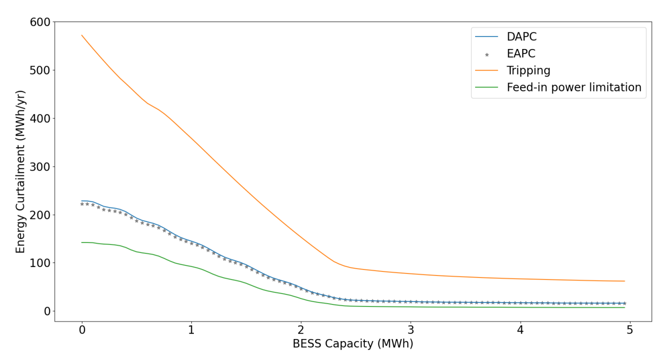

Fig. 10. Annual energy curtailment decrement when installing BESS.

H. Comparison with Volt-Var-Watt method for voltage mitigation

The proposed EAPC method is compared with a local Volt-Var-Watt method that combines Volt-Var and Volt-Watt methods. This is primarily due to the following reasons: i) Limited Impact: The high R/X ratio inherent to the European LV network model, which is typical of many existing networks results in voltage being more sensitive to active power variations compared to reactive power. This significantly limits

TABLE IV
COMPARATIVE RESULTS OF EAPC AND VOLT-VAR-WATT METHOD

Method	Energy curtailment (MWh)	Network losses (MWh)
EAPC	1.05	8
Volt-VAr-Watt	0.50	11.5

Volt-Var's effectiveness, especially during peak PV generation periods around midday, when demand is typically low. ii) Potential for Undervoltage: Aggressively adjusting power factor towards 0.8, especially at lower PV output levels, can risk causing undervoltage issues closer to the substation. While some schemes dynamically vary the target PF, this adds complexity and may not fully resolve the issue. The Volt-Var-Watt method is implemented in two stages. Firstly, the power factor is adjusted to $cos(\phi) = 0.8$ when the PV output surpasses 50% of the nominal power based on the $cos\phi(P)$ (Volt-Var) control [21], [59]. After that, the droop-based APC (Vol-Watt) control is implemented according to Eq (3) to fully ensure overvoltage mitigation. Comparitive results are reported in table IV. Although the Volt-Var-Watt method requires less energy curtailment it increases the network losses by 44% compared to EAPC due to the increased current flow. It is worth mentioning that a higher size of the solar inverter is required to operate with a power factor of 0.8, adding additional expenses to the initial investment of PV systems. Furthermore, this method fails in equitably curtailing energy, impacting the distant prosumers more as they experience the highest voltage along the feeder.

V. Discussion

While this study primarily focuses on developing the EAPC algorithm, we acknowledge the significance of real-world feasibility. To provide a preliminary assessment, we consider the following hardware and communication, and operational framework aspects and limitations of the active power control methods.

A. Hardware

Each prosumer's PV inverter would need capabilities for setpoint reception, securely receiving digitally encoded active power setpoints from the DSO, potentially using a protocol like Modbus TCP/IP or IEC 61850; fast control, adjusting power output quickly enough to respond to setpoint changes within a timeframe of 1-5 seconds, depending on grid stability requirements; and data logging, optional but beneficial for local storage of recent data (setpoints, output, voltage) to aid in diagnostics and system robustness if communication is temporarily lost. DSO control center requires processing power, a server (or cluster for large networks) with sufficient computational resources to perform the power flow and EAPC calculations within the desired 1-minute interval for a network size comparable to the one studied; and data management and security, a robust system for secure data aggregation from smart meters, communication with inverters, and storage/archiving. Cybersecurity considerations are paramount for such a system.

B. Communication

The centralized nature of EAPC requires a reliable and low-latency communication link between the DSO's control center and each prosumer inverter. Potential technologies include powerline communications (PLC) leveraging the existing electrical infrastructure, though bandwidth limitations and susceptibility to noise might need mitigation; cellular networks (4G/5G), offering good coverage but potentially introducing variable latency and cost implications; dedicated RF Mesh Networks designed for smart grid applications, balancing reliability with deployment costs; and fiber optic cable, offering high bandwidth and security, but might only be feasible for new deployments with existing fiber infrastructure. Estimating precise bandwidth depends heavily on the data rate needed for each function. If we assume sending active power setpoints (e.g., a few bytes) to each inverter every minute, with additional bandwidth allocated for infrequent parameter updates and meter data collection, e.g., voltage readings, etc., a rough upper bound on communication requirements might be on the order of 10-50 kbps per prosumer per interval.

C. Operational framework

The proposed EAPC method depends on accurate consumption and generation profiles of prosumers. Smart meters record consumption profiles remotely, providing the utility with precise demand power curves. PV generation profiles can be forecasted using typical generation patterns for each prosumer, adjusted for weather forecasts. By using these profiles, utilities can implement EAPC to create active power setpoints for each prosumer, which is then communicated to them for the upcoming time period.The concept of the framework is illustrated in Fig 11.

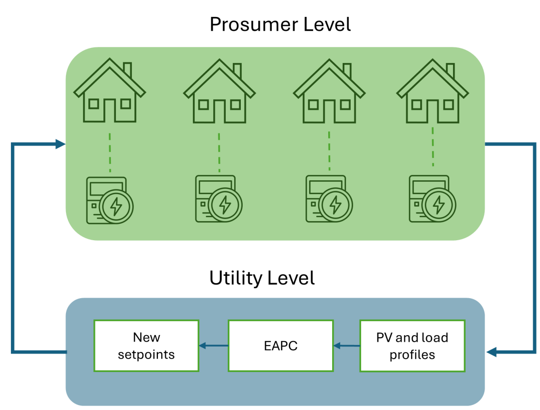

Fig. 11. Conceptual design of the operational framework for the EAPC implementation.

D. Limitations of active power control methods

The active power control methods presented in this paper are effective in mitigating the voltage rise to some extent. However, each method comes with its drawbacks. DAPC and tripping methods, in common, introduce unfairness between the prosumers due to varying curtailments. Table V shows the comparison of the four methods from different perspectives.

TABLE V
COMPARISON OF THE POWER CURTAILMENT METHODS

Methods	Occurrence of voltage violation	Communication Link	Sensitivity to location	Monitoring Req.	Control Structure
EAPC	×	✓	×	High	Centralized
DAPC	×	✓	✓	High	Centralized
Feed-in power	✓	×	×	Low	Local
Tripping	×	×	✓	Low	Local

Unlike DAPC, EAPC is based on SCR which makes it superior in mitigating the location impact and maintaining the voltage within the allowed range. However, both methods require long-range communication and monitoring infrastructure between prosumers, which might be challenging for the DSO. However, considering the advancement in smart grid technologies, implementing these methods is assumed to be less complex in the near future. On the other hand, Feed-power and tripping methods are based on local control, making their implementation more simple. Nevertheless, the main drawback of the Feed-in power method is that it applies a uniform feed-in coefficient, leading to unnecessary curtailment. Moreover, voltage violations might occur under this control method. Therefore, a dynamic feed-in coefficient must be adopted to avoid these drawbacks. In contrast, the tripping method is highly sensitive to the prosumer's location, putting the prosumer at the end of the feeders in a disadvantageous position.

VI. CONCLUSION

While generally, the voltage drop at the end of the LV distribution networks is expected traditionally; overvoltage issues arise with the widespread adoption of distributed resources. Especially in PV-rich distribution networks, conventional solutions to mitigate overvoltage problems introduce unfairness in the amount of energy curtailment for the prosumers located at the end of the feeders. However, this paper proposes a more equitable approach for active power curtailment to mitigate overvoltage while considering the interaction between prosumers and the grid. The proposed approach penalizes the prosumers who fail to satisfy a certain SCR level to support raising self-consumption locally to lower the impact on the grid. The proposed method curtails energy based on the voltage sensitivity matrix that reflects the relation between the power injection and the bus voltage. A comparative analysis of the proposed EAPC and three prevalent methods, feed-in power limitation, inverter tripping, and DAPC, shows that slightly less energy curtailment occurs for penetration levels below 60%; thus, the tripping method is desired because of its simplicity. The feed-in power limitation method does not preserve voltage safety for PV penetration above 80% because it does not consider demand and supply interaction. However, EAPC exhibits reduced sensitivity to the prosumer's location within the feeders while effectively alleviating overvoltage incidents. Additionally, the location sensitivity of EAPC and DAPC is evaluated by moving one prosumer from the feeder's beginning to the end, and the results indicate that only a 4 kWh energy curtailment difference occurred under EAPC. Meanwhile, this value is 40 kWh under DAPC, resulting in a ten times higher curtailment due to the location of the prosumer, proving that EAPC treats prosumers more equitably than DAPC. The opportunity of leveraging BESS to reduce energy loss is also examined. The energy curtailment difference between EAPC and DAPC can be decreased to less than 1.5% annually, without the need to increase the capacity of the BESS. The proposed method would help the prosumers manage their active power and encourage them to achieve high self-consumption. Further research is needed to thoroughly assess the technological and economic tradeoffs involved in deploying EAPC in real-world settings, potentially exploring distributed control strategies to mitigate communication overheads.

REFERENCES

[1] I. Diab, N. Damianakis, G. R. Chandra-Mouli, and P. Bauer, "A shared PV system for transportation and residential loads to reduce curtailment and the need for storage systems," Appl. Energy, vol. 353, no. PB, p. 122131, 2024, doi: 10.1016/j.apenergy.2023.122131.

[2] S. Lin, T. Ma, and M. Shahzad Javed, "Prefeasibility study of a distributed photovoltaic system with pumped hydro storage for residential buildings," Energy Convers. Manag., vol. 222, no. February, p. 113199, Oct. 2020, doi: 10.1016/j.enconman.2020.113199.

[3] R. Khezri, A. Mahmoudi, and D. Whaley, "Optimal sizing and comparative analysis of rooftop PV and battery for grid-connected households with all-electric and gas-electricity utility," Energy, vol. 251, p. 123876, 2022, doi: 10.1016/j.energy.2022.123876.

[4] S. Rahman et al., "Analysis of Power Grid Voltage Stability with High Penetration of Solar PV Systems," IEEE Trans. Ind. Appl., vol. 57, no. 3, pp. 2245–2257, 2021, doi: 10.1109/TIA.2021.3066326.

[5] E. E. E. Ahmed and A. Demirci, "Assessment of overvoltage and power losses in low voltage distribution networks with high photovoltaics penetration based on prosumers' self-consumption," in HORA 2022 - 4th International Congress on Human-Computer Interaction, Optimization and Robotic Applications, Proceedings, 2022, no. 1, pp. 1–4. doi: 10.1109/HORA55278.2022.9800001

[6] E. E. E. Ahmed and G. Poyrazoglu, "Optimizing Distributed Generation Sizing and Siting using Particle Swarm Optimization: A Comparative Study," in Proceedings - 2023 IEEE International Conference on Environment and Electrical Engineering and 2023 IEEE Industrial and Commercial Power Systems Europe, EEEIC / I and CPS Europe 2023, 2023, no. 3, pp. 0–4. doi: 10.1109/EEEIC/ICPSEurope57605.2023.10194717.

[7] M. Shafiullah, S. D. Ahmed, and F. A. Al-Sulaiman, "Grid Integration Challenges and Solution Strategies for Solar PV Systems: A Review," IEEE Access, vol. 10, pp. 52233–52257, 2022, doi: 10.1109/ACCESS.2022.3174555.

[8] H. Ravindra, M. O. Faruque, P. McLaren, K. Schoder, M. Steurer, and R. Meeker, "Impact of PV on distribution protection system," 2012 North Am. Power Symp. NAPS 2012, pp. 1–6, 2012, doi: 10.1109/NAPS.2012.6336409.

[9] M. Hasheminamin, V. G. Agelidis, V. Salehi, R. Teodorescu, and B. Hredzak, "Index-Based Assessment of Voltage Rise and Reverse Power Flow Phenomena in a Distribution Feeder under High PV Penetration," IEEE J. Photovoltaics, vol. 5, no. 4, pp. 1158–1168, 2015, doi: 10.1109/JPHOTOV.2015.2417753.

[10] J. Von Appen, M. Braun, T. Stetz, K. Diwold, and D. Geibel, "Time in the sun: The challenge of high PV penetration in the German electric grid," IEEE Power Energy Mag., vol. 11, no. 2, pp. 55–64, 2013, doi: 10.1109/MPE.2012.2234407.

[11] J. P. Holguin, D. C. Rodriguez, and G. Ramos, "Reverse Power Flow (RPF) Detection and Impact on Protection Coordination of Distribution Systems," IEEE Trans. Ind. Appl., vol. 56, no. 3, pp. 2393–2401, 2020, doi: 10.1109/TIA.2020.2969640.

[12] M. A. Ghasemi and M. Parniani, "Prevention of distribution network overvoltage by adaptive droop-based active and reactive power control of PV systems," Electr. Power Syst. Res., vol. 133, pp. 313–327, 2016, doi: 10.1016/j.epsr.2015.12.030.

[13] T. R. de Barros, J. A. G. Archetti, M. Mattos, L. W. de Oliveira, and J. G. Oliveira, "Optimization algorithm associated with local and coordinated controls of distributed energy resources to meet technical and economic criteria," Electr. Power Syst. Res., vol. 226, no. October 2023, p. 109880, 2024, doi: 10.1016/j.epsr.2023.109880.

[14] W. Group, IEEE Application Guide for IEEE Std 1547, IEEE Standard for Interconnecting Distributed Resources with Electric Power Systems, no. April. 2008.

[15] Z. Wang, X. Yu, Y. Mu, and H. Jia, "A distributed Peer-to-Peer energy transaction method for diversified prosumers in Urban Community Microgrid System," Applied Energy, vol. 260. 2020. doi: 10.1016/j.apenergy.2019.114327.

[16] C. Yin and F. Li, "Reactive power control strategy for inhibiting transient overvoltage caused by commutation failure," IEEE Trans. Power Syst., vol. 36, no. 5, pp. 4764–4777, 2021, doi: 10.1109/TPWRS.2021.3063276.

[17] E. E. Pompodakis, I. A. Drougakis, I. S. Lelis, and M. C. Alexiadis, "Photovoltaic systems in low-voltage networks and overvoltage correction with reactive power control," IET Renew. Power Gener., vol. 10, no. 3, pp. 410–417, 2016, doi: 10.1049/iet-rpg.2014.0282.

[18] A. Safayet, P. Fajri, and I. Husain, "Reactive Power Management for Overvoltage Prevention at High PV Penetration in a Low-Voltage Distribution System," IEEE Trans. Ind. Appl., vol. 53, no. 6, pp. 5786–5794, 2017, doi: 10.1109/TIA.2017.2741925.

[19] A. M. Howlader, S. Sadoyama, L. R. Roose, and Y. Chen, "Active power control to mitigate voltage and frequency deviations for the smart grid using smart PV inverters," Appl. Energy, vol. 258, no. April 2019, p. 114000, 2020, doi: 10.1016/j.apenergy.2019.114000.

[20] R. Tonkoski, L. A. C. Lopes, and T. H. M. El-Fouly, "Coordinated active power curtailment of grid connected PV inverters for overvoltage prevention," IEEE Trans. Sustain. Energy, vol. 2, no. 2, pp. 139–147, 2011, doi: 10.1109/TSTE.2010.2098483.

[21] A. I. Nousdilis, G. C. Christoforidis, and G. K. Papagiannis, "Active power management in low voltage networks with high photovoltaics penetration based on prosumers' self-consumption," Appl. Energy, vol. 229, no. April 2018, pp. 614–624, Nov. 2018, doi: 10.1016/j.apenergy.2018.08.032.

[22] G. C. Kryonidis, E. O. Kontis, A. I. Chrysochos, C. S. Demoulias, and G. K. Papagiannis, "A Coordinated Droop Control Strategy for Overvoltage Mitigation in Active Distribution Networks," IEEE Trans. Smart Grid, vol. 9, no. 5, pp. 5260–5270, 2018, doi: 10.1109/TSG.2017.2685686.

[23] A. M. S. Alonso, L. D. O. De Oro Arenas, D. I. Brandao, E. Tedeschi, and F. P. Marafao, "Integrated Local and Coordinated Overvoltage Control to Increase Energy Feed-In and Expand der Participation in Low-Voltage Networks," IEEE Trans. Sustain. Energy, vol. 13, no. 2, pp. 1049–1061, 2022, doi: 10.1109/TSTE.2022.3146196.

[24] R. Wagle, P. Sharma, C. Sharma, and M. Amin, "Optimal power flow based coordinated reactive and active power control to mitigate voltage violations in smart inverter enriched distribution network," Int. J. Green Energy, vol. 21, no. 2, pp. 359–375, 2024, doi: 10.1080/15435075.2023.2196324.

[25] Y. Z. Gerdroodbari, R. Razzaghi, and F. Shahnia, "Decentralized Control Strategy to Improve Fairness in Active Power Curtailment of PV Inverters in Low-Voltage Distribution Networks," IEEE Trans. Sustain. Energy, vol. 12, no. 4, pp. 2282–2292, 2021, doi: 10.1109/TSTE.2021.3088873.

[26] L. Collins and J. K. Ward, "Real and reactive power control of distributed PV inverters for overvoltage prevention and increased renewable generation hosting capacity," Renew. Energy, vol. 81, pp. 464–471, 2015, doi: 10.1016/j.renene.2015.03.012.

[27] T. T. Mai, N. A. N. M. M. Haque, H. T. Vo, and P. H. Nguyen, "Coordinated active and reactive power control for overvoltage mitigation in physical LV microgrids," J. Eng., vol. 2019, no. 18, pp. 5007–5011, 2019, doi: 10.1049/joe.2018.9355.

[28] L. Cheng, Y. Chang, and R. Huang, "Mitigating Voltage Problem in Distribution System with Distributed Solar Generation Using Electric Vehicles," IEEE Trans. Sustain. Energy, vol. 6, no. 4, pp. 1475–1484, 2015, doi: 10.1109/TSTE.2015.2444390.

[29] C. L. Masters, "Voltage rise the big issue when connecting embedded generation to long 11 kv overhead lines," Power Eng. J., vol. 16, no. 1, pp. 5–12, 2002, doi: 10.1049/pe:20020101.

[30] J. Lazo and D. Watts, "Stochastic model for active distribution networks planning: An analysis of the combination of active network management schemes," Renew. Sustain. Energy Rev., vol. 191, no. December 2023, p. 114156, 2024, doi: 10.1016/j.rser.2023.114156.

[31] M. M. V. M. Ali, P. H. Nguyen, W. L. Kling, A. I. Chrysochos, T. A. Papadopoulos, and G. K. Papagiannis, "Fair power curtailment of distributed renewable energy sources to mitigate overvoltages in low-voltage networks," 2015 IEEE Eindhoven PowerTech, PowerTech 2015, no. 608998, 2015, doi: 10.1109/PTC.2015.7232796.

[32] S. M. Alizadeh, C. Ozansoy, and T. Alpcan, "The impact of X/R ratio on voltage stability in a distribution network penetrated by wind farms," 2016 Australas. Univ. Power Eng. Conf., pp. 1–6, 2016, doi: 10.1109/aupec.2016.7749289.

[33] X. Su, L. Fang, J. Yang, F. Shahnia, Y. Fu, and Z. Y. Dong, "Spatial-Temporal Coordinated Volt/Var Control for Active Distribution Systems," IEEE Trans. Power Syst., vol. PP, pp. 1–11, 2024, doi: 10.1109/TPWRS.2024.3370935.

[34] S. Paudyal, B. P. Bhattarai, R. Tonkoski, S. Dahal, and O. Ceylan, "Comparative Study of Active Power Curtailment Methods of PVs for Preventing Overvoltage on Distribution Feeders," IEEE Power Energy Soc. Gen. Meet., vol. 2018-Augus, pp. 1–5, 2018, doi: 10.1109/PESGM.2018.8585526.

[35] A. T. Procopiou, K. Petrou, L. F. Ochoa, T. Langstaff, and J. Theunissen, "Adaptive decentralized control of residential storage in pv-rich mv-lv networks," IEEE Trans. Power Syst., vol. 34, no. 3, pp. 2378–2389, 2019, doi: 10.1109/TPWRS.2018.2889843.

[36] S. Weckx, C. Gonzalez, and J. Driesen, "Combined central and local active and reactive power control of PV inverters," IEEE Trans. Sustain. Energy, vol. 5, no. 3, pp. 776–784, 2014, doi: 10.1109/TSTE.2014.2300934.

[37] S. Alyami, Y. Wang, C. Wang, J. Zhao, and B. Zhao, "Adaptive real power capping method for fair overvoltage regulation of distribution networks with high penetration of PV systems," IEEE Trans. Smart Grid, vol. 5, no. 6, pp. 2729–2738, 2014, doi: 10.1109/TSG.2014.2330345.

[38] F. Olivier, P. Aristidou, D. Ernst, and T. Van Cutsem, "Active Management of Low-Voltage Networks for Mitigating Overvoltages Due to Photovoltaic Units," IEEE Trans. Smart Grid, vol. 7, no. 2, pp. 926–936, 2016, doi: 10.1109/TSG.2015.2410171.

[39] A. Latif, W. Gawlik, and P. Palensky, "Quantification and Mitigation of Unfairness in Active Power Curtailment of Rooftop Photovoltaic Systems Using Sensitivity Based Coordinated Control," Energies, vol. 9, no. 6, 2016, doi: 10.3390/en9060436.

[40] A. Samadi, R. Eriksson, L. Söder, B. G. Rawn, and J. C. Boemer, "Coordinated active power-dependent voltage regulation in distribution grids with PV systems," IEEE Trans. Power Deliv., vol. 29, no. 3, pp. 1454–1464, 2014, doi: 10.1109/TPWRD.2014.2298614..

[41] K. Chatchairungruang and S. Suwankawin, "Peak-shaving of feed-in PV power for residential PV-battery system with added feedback-adjustment scheme," ECTI-CON 2021 - 2021 18th Int. Conf. Electr. Eng. Comput. Telecommun. Inf. Technol. Smart Electr. Syst. Technol. Proc., pp. 192–195, 2021, doi: 10.1109/ECTI-CON51831.2021.9454817.

[42] H. Ruf, "Limitations for the feed-in power of residential photovoltaic systems in Germany – An overview of the regulatory framework," Sol. Energy, vol. 159, no. October 2017, pp. 588–600, 2018, doi: 10.1016/j.solener.2017.10.072.

[43] S. M. Tercan, A. Demirci, E. Gokalp, and U. Cali, "Maximizing self-consumption rates and power quality towards two-stage evaluation for solar energy and shared energy storage empowered microgrids," J. Energy Storage, vol. 51, no. June 2021, p. 104561, 2022, doi: 10.1016/j.est.2022.104561.

[44] R. Tonkoski, L. A. C. Lopes, and T. H. M. EL-Fouly, "Droop-based active power curtailment for overvoltage prevention in grid connected PV inverters," IEEE Int. Symp. Ind. Electron., no. 2388, pp. 2388–2393, 2010, doi: 10.1109/ISIE.2010.5637511.

[45] R. Tonkoski, L. A. C. Lopes, and T. H. M. El-Fouly, "Coordinated active power curtailment of grid connected PV inverters for overvoltage prevention," IEEE Trans. Sustain. Energy, vol. 2, no. 2, pp. 139–147, 2011, doi: 10.1109/TSTE.2010.2098483.

[46] F. Ni, P. H. Nguyen, J. F. G. Cobben, H. E. Van den Brom, and D. Zhao, "Three-phase state estimation in the medium-voltage network with aggregated smart meter data," Int. J. Electr. Power Energy Syst., vol. 98, no. February, pp. 463–473, 2018, doi: 10.1016/j.ijepes.2017.12.033.

[47] A. I. Nousdilis, A. I. Chrysochos, G. K. Papagiannis, and G. C. Christoforidis, "The impact of Photovoltaic Self-Consumption Rate on voltage levels in LV distribution grids," 2017 11th IEEE Int. Conf. Compat. Power Electron. Power Eng. CPE-POWERENG 2017, pp. 650–655, 2017, doi: 10.1109/CPE.2017.7915249.

[48] S. van der Stelt, T. AlSkaif, and W. van Sark, "Techno-economic analysis of household and community energy storage for residential prosumers with smart appliances," Appl. Energy, vol. 209, no. August 2017, pp. 266–276, 2018, doi: 10.1016/j.apenergy.2017.10.096.

[49] L. Thurner et al., "Pandapower - An Open-Source Python Tool for Convenient Modeling, Analysis, and Optimization of Electric Power Systems," IEEE Trans. Power Syst., vol. 33, no. 6, pp. 6510–6521, 2018, doi: 10.1109/TPWRS.2018.2829021.

[50] M. G. Kashani, M. Mobarrez, and S. Bhattacharya, "Smart Inverter Volt-Watt Control Design in High PV-Penetrated Distribution Systems," IEEE Trans. Ind. Appl., vol. 55, no. 2, pp. 1147–1156, 2019, doi: 10.1109/TIA.2018.2878844.

[51] S. Yoshizawa et al., "Voltage-Sensitivity-Based Volt-VAR-Watt Settings of Smart Inverters for Mitigating Voltage Rise in Distribution Systems," IEEE Open Access J. Power Energy, vol. 8, no. September, pp. 584–595, 2021, doi: 10.1109/OAJPE.2021.3125013.

[52] M. Z. Liu et al., "On the Fairness of PV Curtailment Schemes in Residential Distribution Networks," IEEE Trans. Smart Grid, vol. 11, no. 5, pp. 4502–4512, 2020, doi: 10.1109/TSG.2020.2983771.

[53] D. Gebbran, S. Mhanna, Y. Ma, A. C. Chapman, and G. Verbič, "Fair coordination of distributed energy resources with Volt-Var control and PV curtailment," Appl. Energy, vol. 286, no. January, 2021, doi: 10.1016/j.apenergy.2021.116546.

[54] S. Poudel, M. Mukherjee, and A. P. Reiman, "A Fairness-Based Distributed Energy Coordination for Voltage Regulation in Distribution Systems," IEEE Green Technol. Conf., vol. 2022-April, pp. 45–50, 2022, doi: 10.1109/GreenTech52845.2022.9772030.

[55] C. L. Dewangan, S. Chakrabarti, S. N. Singh, and M. Sharma, "A Fair Incentive Scheme for Participation of Smart Inverters in Voltage Control," IEEE Trans. Ind. Informatics, vol. 18, no. 1, pp. 656–665, 2022, doi: 10.1109/TII.2021.3053757.

[56] M. Mukherjee, S. Poudel, R. Sadnan, T. E. Slay, and A. P. Reiman, "Enabling Fairness in Distributed PV Curtailment for Voltage Regulation: A Comparative Analysis," 2024 IEEE Power Energy Soc. Innov. Smart Grid Technol. Conf. ISGT 2024, pp. 1–5, 2024, doi: 10.1109/ISGT59692.2024.10454182.

[57] "IEEE PES Distribution test feeders. The IEEE European Low Voltage Test Feeder." https://cmte.ieee.org/pes-testfeeders/resources/ (accessed Mar. 03, 2024).

[58] M. B. Stackhouse Jr PW, Zhang T, Westberg D, Barnett AJ, Bristow T and H. JM, "POWER Release 8 (with GIS Applications) Methodology," 2023. https://power.larc.nasa.gov/data-access-viewer/

[59] E. Demirok, P. C. González, K. H. B. Frederiksen, D. Sera, P. Rodriguez, and R. Teodorescu, "Local Reactive Power Control Methods for Overvoltage Prevention of Distributed Solar Inverters in Low-Voltage Grids," IEEE J. Photovoltaics, vol. 1, no. 2, pp. 174–182, Oct. 2011, doi: 10.1109/JPHOTOV.2011.2174821.

Eihab E.E. Ahmed (Student member, IEEE) received the B.Sc. from the Department of Electrical Engineering, Yildiz Technical University, Istanbul, Turkey, in 2022. He is pursuing his master's program in the Department of Electric and Electronic Engineering at Ozyegin University. Furthermore, he is a researcher and teaching assistant in the same department. His research interests include power system optimization, distributed renewable energy systems, smart grid applications, electric vehicles, and energy storage systems. He has published several papers related to his research areas.

Alpaslan Demirci (Member, IEEE) received the B.Sc. degree in electrical and electronics engineering from Sakarya University, Turkey, the B.Sc. and M.Sc. degrees in electrical education from Marmara University, İstanbul, Turkey, in 2007 and 2011, respectively, and the Ph.D. degree in electrical engineering from the Graduate School of Science and Engineering, Yildiz Technical University (YTU), İstanbul, in 2023. He is currently an Associate Professor with the Department of Electrical Engineering, YTU. His research interests include power system optimization methods, distributed renewable energy systems, energy economics, electric vehicles, and energy storage systems. He has published several articles related his research areas.

Gokturk Poyrazoglu (Senior Member, IEEE) received an M.Sc. and Ph.D. in Electrical Engineering from the State University of New York at Buffalo in 2013 and 2015, respectively. He worked at Alevo Analytics and Electric Power Research Institute (EPRI) in Charlotte, NC. Since 2017, he has been a faculty member at Ozyegin University. He is the Department Head of the Electrical and Electronics Engineering Department and the Director of the Grid Operations and Planning Laboratory at Ozyegin University. He received the Turkish Council of Higher Education 2022 Outstanding Achievement on University-Business World Cooperation Award

Saeed D. Manshadi (Senior Member, IEEE) received the B.S. degree in electrical engineering from the University of Tehran, Tehran, Iran, in 2012, the M.S. degree in electrical engineering from the University at Buffalo, State University of New York, Buffalo, NY, USA, in 2014, and the Ph.D. degree in electrical engineering from Southern Methodist University, Dallas, TX, USA, in 2018. He was a Postdoctoral Fellow with the University of California, Riverside, Riverside, CA, USA. He is currently an Assistant Professor with the Department of Electrical and Computer Engineering, San Diego State University, San Diego, CA, USA. His research interests include smart grids, microgrids, integrating renewable and distributed resources, and power system operation and planning. Dr. Manshadi is an Associate Editor for the IEEE TRANSACTIONS ON VEHICULAR TECHNOLOGY.